College of Basic Education Research Journal

www.berj.mosuljournals.com

Green Synthesis ZnO NPs and Their Effects on Plant Growing

Himdad H. Azeez
Physics Department, College of Education/Shaqlawa, Salahaddin University-Erbil, Iraq.
Hiwa H. Hasan
Biology Department, College of Education/Shaqlawa, Salahaddin University-Erbil, Iraq.
Dr. Hawbash H. Karim
Department of Physics, Faculty of Science and Health, Koya University, Koya KOY45, Kurdistan Region - F.R. Iraq

Article Information

Article history:
Received: January 25,2024
Reviewer: March 17,2024
Accepted: March 27,2024
Available online

Keywords:
Green synthesis; ZnO NPs; Plant Growing; XRD and EDX techniques

Correspondence:
himdad.azeez@su.edu.krd
hiwa.h.hasan@su.edu.krd
hawbash.hamadamin@koyauniversity.org

Abstract

This study investigates the production of ZnO NPs by the green method and the effects of these nanoparticles on plant growth. Artemisia abrotanum L. leaf extract was used as a chelating and capping agent. It was found that the Artemisia abrotanum L. leaf extract has the potential to biosynthesize ZnO NPs. FT-IR, UV-Vis, XRD, FE-SEM, and EDX techniques were utilized in this study. The energy band gap of ZnO-NPs was calculated to be around 2.48 eV. The average size crystal structure of NPs was 50.29 nm, as confirmed by XRD. However, the ZnO nanoparticles have a nanorod shape with a size of 66.93 nm, as evaluated by FE-SEM, and the EDX confirmed that the sample is pure ZnO nanoparticles. In addition, The nanoparticles were used to grow Lepidium sativum L. plants. The total growth of Lepidium sativum L. dramatically increased with the use of ZnO NPs, and the content of natural dyes like chlorophyll a and b increased twofold compared to the control. It was explained that zinc oxide nanoparticles are a good candidate for growing plants instead of chemical fertilizers.

ISSN: 1992 – 7452

التوليف الأخضر لأكسيد الزنك جسيمة نانوية وتأثيراته على نمو النبات

هيمداد حمد عزيز
قسم الفيزياء، كلية التربية/شقلاوة، جامعة صلاح الدين-أربيل، العراق

هيوا حسين حسن
قسم الأحياء، كلية التربية/شقلاوة، جامعة صلاح الدين-أربيل، العراق

هاوبەش حمدامين كريم
قسم الفيزياء، كلية العلوم والصحة، جامعة كوية، كوية KOY45، إقليم كوردستان - ف.ر. العراق

ملخص البحث:

تتناول هذه الدراسة إنتاج جزيئات أكسيد الزنك النانوية بالطريقة الخضراء وتأثير هذه الجسيمات النانوية على نمو النبات. تم استخدام مستخلص أ وراق L *Artemisia abrotanum*. كعامل خالب وتغطية. تم العثور على مستخلص أوراق L *Artemisia abrotanum*. لديه القدرة على التخليق الحيوي لـ ZnO NPs. تم استخدام تقنيات FT-IR وUV–Vis وXRD وFE-SEM وEDX في هذه الدراسة. تم حساب فجوة طاقة ZnO NPs بحوالي ٢,٤٨ فولت. كان متوسط التركيب البلوري جزيئات النانوية لحجم 50.29 نانومتر وأكده XRD. ومع ذلك، فإن جزيئات أكسيد الزنك النانوية لها شكل قضيب نانو بحجم ٦٦,٩٣ نانومتر تم تقييمها بواسطة FE-SEM، وأكد EDX أن العينة عبارة عن جزيئات أكسيد الزنك النانوية النقية. بالإضافة إلى ذلك، تم استخدام الجسيمات النانوية في زراعة نبات (*Lepidium sativum*). زاد النمو الكلي لـ (L *Lepidium sativum*) بشكل كبير مع استخدام ZnO NPs، كما زاد محتوى الأصباغ الطبيعية مثل الكلوروفيل a وb بمقدار ضعفين مقارنة بالسيطرة. وقد تم توضيح أن جزيئات أكسيد الزنك النانوية تعتبر مرشحاً جيداً لزراعة النباتات بدلاً من الأسمدة الكيماوية.

الكلمات المفتاحية: التوليف الأخضر. جزيئات أكسيد الزنك النانوية؛ زراعة النباتات; تقنيات ئيكس ار دى و إي دي إكس.

I. INTRODUCTION

Using materials and machines at the nanoscale is known as nanotechnology (Vidya et al., 2013b). Nanotechnology has numerous applications in various fields including medicine, agriculture, pharmacy, and renewable energy. Nanoparticles are particles that measure between 1 and 100 nm in size (Sadatzadeh et al., 2018). These nanoparticles can have various shapes. Materials or particles at this scale exhibit different properties compared to bulk materials, such as electrical, chemical, optical, and thermal properties (Bala et al., 2015, Karim and Omar, 2020). Furthermore, nanoparticles have a large surface area in relation to their volume. This occurs because when the number of surface atoms exceeds the number of atoms within the particle's volume, the particle size decreases and its surface energy increases (Sharma et al., Barman, 2021).

The zinc oxide nanoparticles have attracted researchers due to their incredible applications in various fields, including dental care, cosmetics, agriculture, solar cells, and water purification (Narayana et al., 2018, Mahdi et al., 2020). Furthermore, zinc oxide exhibits excellent specifications such as conductivity and transparency. As a semiconductor, zinc oxide has a crystal structure that classifies it as an n-type semiconductor with a wide band gap (Sagar Raut and Thorat, 2015). This compound involves the elements zinc and oxygen, which are located in the second and sixth groups of the periodic table respectively (Narayana et al., 2018).

ZnO nanoparticles can be produced using various techniques, including chemical, physical, and environmentally friendly methods (Hiremath et al., 2013, Hedayati, 2015). Unlike chemical and physical synthesis, the use of plants for nanoparticle synthesis is unique and offers an affordable and environmentally friendly option (Senthilkumar et al., 2017, Olajire and Adesina, 2017). Moreover, the use of plants allows for easy scaling up of production without the need for hazardous chemicals, high pressures, or high temperatures (Devi and Gayathri, 2014, Behzadi et al., 2022).

In this study, ZnO nanoparticles were synthesized using green synthesis, specifically by utilizing the leaf extract of *Artemisia abrotanum L.* and zinc nitrate hexahydrate. These zinc oxide nanoparticles were then utilized as a fertilizer.

II. METHOD AND MATERIALS

A. Sample Preparation

In this study, fresh leaves of *Artemisia abrotanum L*. were collected in Lass Village, Shaqlawa, Erbil Government, Iraqi Kurdistan region. The following equipment was used: a hotplate stirrer, zinc nitrate hexahydrate, beakers, filter paper, an oven, a mortar, and a pestle. First, the fresh leaves of Artemisia abrotanum L. were placed into the mortar and ground into a paste using the pestle. Then, 6 g of the paste was mixed with 100 mL of distilled water in a beaker. The mixture was heated and stirred at 70°C for one hour. Subsequently, the product was filtered using filter paper. Next, 30 mL of the plant extract was heated at 70°C on the hot plate and stirrer. Afterwards, 3 g of zinc nitrate hexahydrate was added to the heated extract. The mixture was further heated and stirred until it formed a paste. The paste was then burned at 350°C for 2 hours, resulting in the formation of ZnO NPs powder.

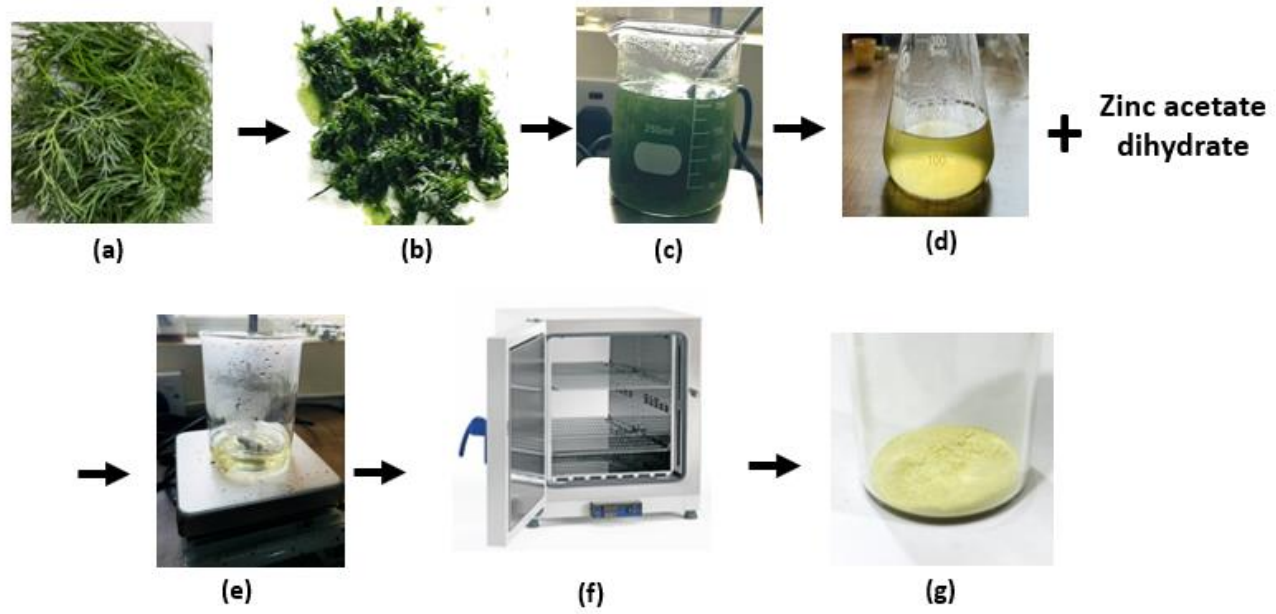

Figure 1.(a) Washing leaves of Artemisia abrotanum L., (b) The leaves being crushed by mortar and pestle, (c) The paste mixed with distilled water was heated and stirred at 70°C, (d) Filtration of the product and mixing it with zinc acetate dihydrate, (e) The mixture was heated and stirred until it became a paste, (f) Burning the paste at 350°C, and (g) Obtained ZnO NPs powder.

B. Application of Synthesized Nanoparticles in Plant Growth

Four soil samples were prepared for this study. Seeds of *Lepidium sativum L*. were then used and planted in these samples. Meanwhile, 3 gm of ZnO NPs were mixed with 3 L of tap water. Two of the samples were watered with the zinc oxide nanoparticles solution, while the other two were watered with tap water. After a period of two weeks, the results were observed.

C. Morphological Study

Plant height and stem diameter were measured at the end of the experiment. In addition, petiole and leaf length were also measured.

D. Determination of The Dye Content in Plant Leaf

To create the extract, dimethyl sulfoxide (DMSO) and 0.1 g of plant material were combined. After being left at room temperature for approximately an hour in the dark, the samples were incubated at 65 °C (water bath) for 30 minutes. The amount of chlorophyll dyes was measured using a UV/VIS8453 spectrophotometer at the following wavelengths: 663 nm for chlorophyll a, 645 nm for chlorophyll b, 470 nm for carotenoids, and 534 nm for anthocyanins. The Arnon formula (1949), modified by Richardson et al. (Richardson et al., 2002), was used to determine the amount of vegetable dyes present. The dosage of individual dyes was measured in mg/g of fresh weight.

III. RESULTS AND DISCUSSION

A. Characterization of plant extract

Researchers are currently creating customized nanoparticles by synthesizing them using specific phytochemicals derived from plants. These phytochemicals, found within the plant extract, are responsible for transforming metal ions into metal nanoparticles. As a result, the plant extract acts as both a stabilizing and reducing agent in this process. The progress of this reaction is monitored using UV-visible spectroscopy.

UV-Vis analysis of *Artemisia abrotanum* L. leaf extract

Before using *Artemisia abrotanum* L. leaf extract, it must be characterized by UV-Vis spectroscopy to determine the presence of phytochemicals within the plant. These

phytochemicals function as reducing and stabilizing agents for nanoparticle synthesis (Reddy et al., 2021).

The UV-Vis spectra of *Artemisia abrotanum* L. leaf extract are shown in Figure 2. The highest peaks at 262 nm and 326 nm represent phenolic components and flavonoids, respectively, in *Artemisia abrotanum* L. leaf extract. *Artemisia abrotanum* L. leaf extract contains flavonoids, polyphenols, carotenoids, lipids, polysaccharides, tannins, free organic acids, and essential oils. This indicates that this plant is rich in OH groups, which are believed to be potential bio-reducing and stabilizing agents for nanoparticle synthesis(Lee et al., 2013).

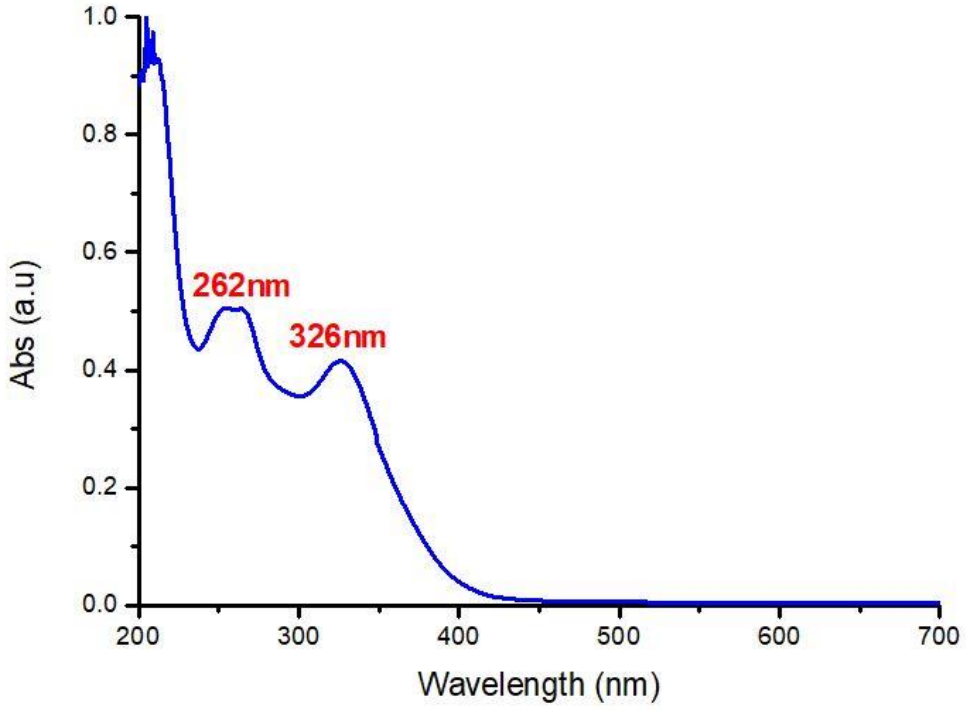

Figure 2. UV-Vis spectra of *Artemisia abrotanum* L. leaf extract.

FT-IR analysis of *Artemisia abrotanum* L. leaf extract

The FT-IR spectra obtained from the leaf extract of *Artemisia abrotanum* L., as shown in Figure 3, display a wide range of distinctive peaks covering the entire spectral range. In the field of Fourier-transform infrared (FT-IR) spectroscopy, these spectra are traditionally divided into two main regions: the functional group region, which spans the

wavenumber range from 1800 to 4000 cm-1, and the fingerprint region, which extends from 0 to 1500 cm^{-1}. Within the observed FT-IR spectrum, there are several prominent peaks that can be identified. Specifically, the bands occurring between 1600 cm^{-1} and 3200 cm^{-1} indicate the stretching vibrations of tertiary amide C=O bonds and the O-H stretching vibrations of phenolic groups. Furthermore, the presence of bands at 1645 cm^{-1} is attributed to the stretching vibrations of tertiary amide C=O bonds, which is a characteristic feature as reported by Isaac et al. in 2013(Isaac et al., 2013).

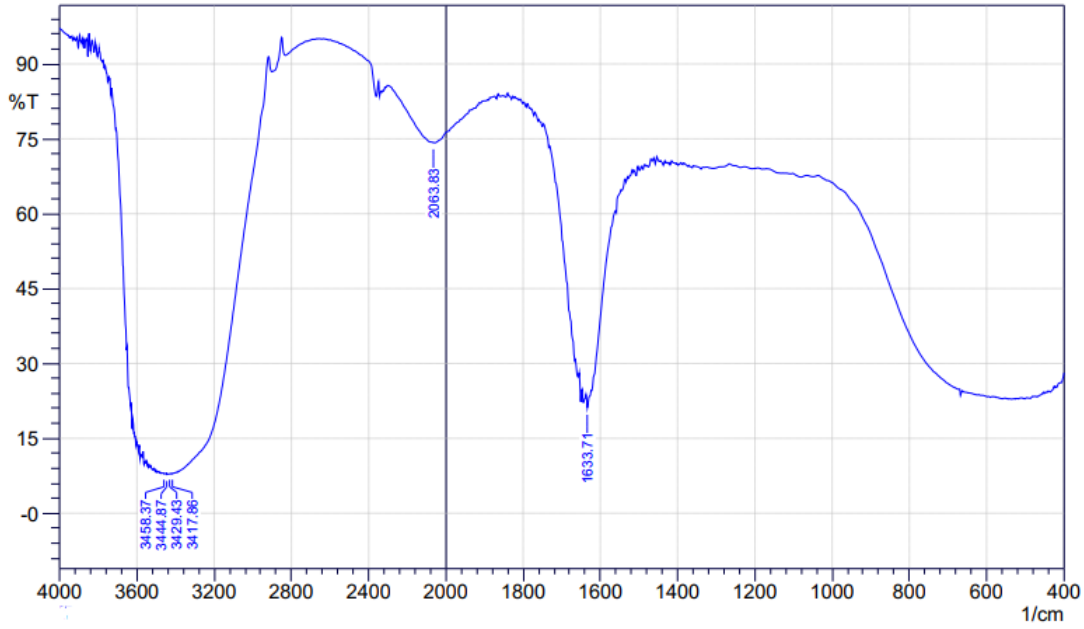

Figure 3. FT-IR spectra of *Artemisia abrotanum* L. leaf extract.

B. Characterization of ZnO NPs

UV-Vis analysis of ZnO NPs

In response to electromagnetic waves, surface plasmon resonance, which collects conduction band electron oscillations, showed a peak absorption in UV-Vis spectroscopy, indicating the production of nanoparticles and the reduction of metal ions. (Evanoff Jr and Chumanov, 2005).

The peak at 373 nm observed by UV-Vis spectroscopy (Figure 4) was typical of ZnO NPs. The surface plasmon resonance (SPR) was responsible for this, and the sharper peak proved the formation of mono dispersed ZnO NPs (Pai et al., 2019). The absorption peak maxima for ZnO NPs are typically between 300 and 380 nm (Varadavenkatesan et al., 2019). The calculated value is lower than 380 nm and exhibits a blue shift in excitonic absorption.

ZnO NPs are known for having a peak at 373 nm, which was observed by UV-Vis spectroscopy (Figure 3). This was caused by the surface plasmon resonance (SPR), and the sharper peak indicated the formation mono dispersed ZnO NPs (Pai et al., 2019). ZnO NPs typically have absorbance peak maxima between 300 and 380 nm (Varadavenkatesan et al., 2019). The computed value shows an excitonic absorption shift to the blue and is less than 380 nm.

The straightforward band-gap energy *E (g)* for ZnO NPs is obtained by fitting the reflection data to the straight transform formula $\alpha hv = A(hv - E_g)^n$, where α is the absorption coefficient, *hv* is the photon energy, *E (g)* is the straight band-gap, *A* is the absorbance, and the power n is an integer for the direct band gap n=1/2. Extending the rectilinear component of $(\alpha hv)^2$ *vs hv* to the x-axis provides information about the exact band gap magnitude.

Figure 4 shows that the straight band gap for ZnO NPs is 2.48 eV. Utilizing plant extract is expected to result in a decrease in the band-gap, and for the greenly produced nanoparticles, this result does not conflict with the spatial quantum confinement effects because some plant extract components cover/modify the surface and reduce the band-gap of the nanoparticles (Khan et al., 2019). Nanoparticles produced through biosynthesis are typically more reactive than identical nanoparticles produced through other methods (Pantidos and Horsfall, 2014).

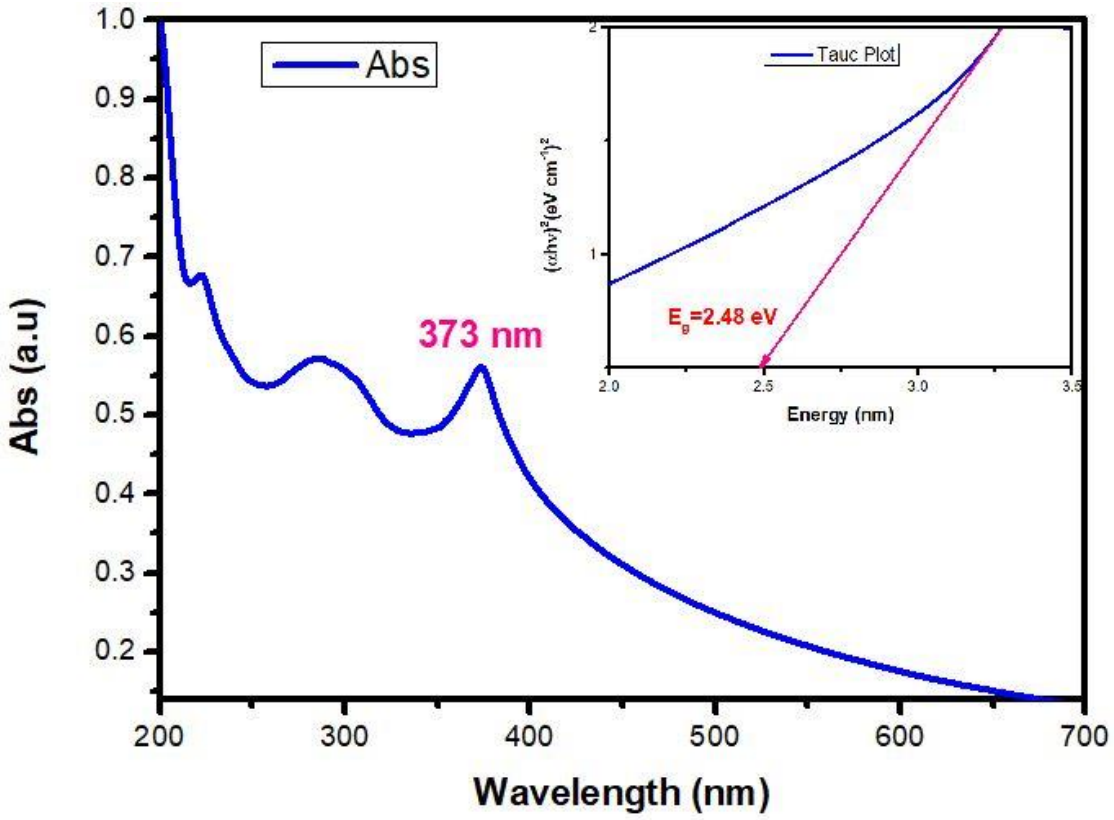

Figure 4. UV-Vis spectroscopy of ZnO NPs.

FT-IR analysis of ZnO NPs

In Figure 5, we present the Fourier-transform infrared (FT-IR) spectrum. This spectrum has been used to rigorously assess the purity and composition of biosynthesized zinc oxide nanoparticles (ZnO NPs). The absence of any discernible peaks within the monitoring range clearly demonstrates the remarkable purity achieved through our environmentally friendly synthesis approach. This unequivocally shows that the "green" method used to produce ZnO NPs has successfully yielded highly pure nanoparticles.

Upon closer examination of the FT-IR spectrum, we can observe specific vibrational signatures that are associated with the zinc and oxygen bonds. These signatures manifest as a distinctive peak at 435 cm^{-1}, which has been previously reported by (Yuvakkumar et al., 2015, Bhuyan et al., 2015). Further analysis of the spectrum reveals additional prominent peaks. One notable band is observed at 1384 cm^{-1}, and it is attributed

to the C–O stretching of the carboxylic acid group. This finding is consistent with the existing literature on these chemical bonds. Additionally, the spectrum exhibits a discernible peak at 1647 cm^{-1}, which indicates the –C=C– stretching vibrations commonly found in aromatic compounds, as reported by (Hu et al., 2019). We also observe a striking and relatively wide band at 3498 cm^{-1}, corresponding to the O-H stretching vibrations associated with phenolic compounds, as reported by (Ganesh et al., 2019). This observation provides valuable insight into the presence of these chemical constituents in our synthesized ZnO NPs.

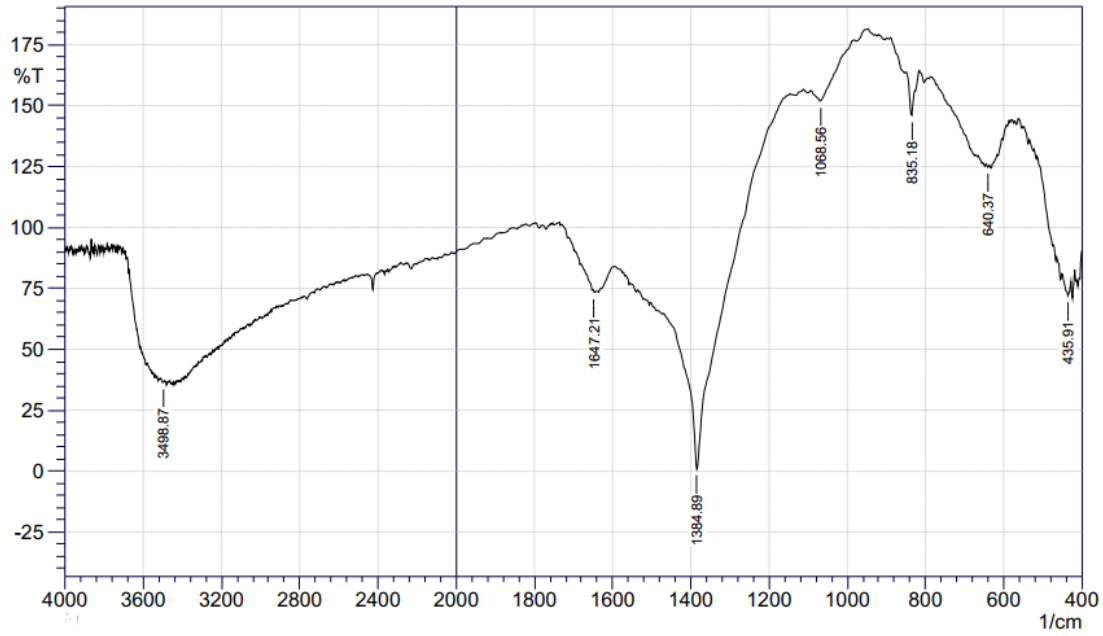

Figure 5. FT-IR spectrum of ZnO NPs.

XRD analysis of ZnO NPs

X-ray diffraction spectra (Figure 6) show eleven peaks at 31.77°, 34.42°, 36.25°, 47.53°, 56.56°, 62.85°, 66.36°, 67.91°, 69.04°, 72.59°, and 76.96°, which correspond to the (100), (002), (101), (102), (110), (103), (200), (112), (201), (004), and (202) planes. This spectrum corresponds to JCPDS card No. 89-0510, which represents the hexagonal Wurtzite crystal structure of ZnO NPs. The crystal size of Zinc Oxide nanoparticles was determined using the (Debye-Scherrer) equation: $D=k\lambda/\beta \cos\theta$, where D represents the crystalline size, k is the shape factor equal to 0.9, λ is the X-ray wavelength (λ=0.154 nm) for Cu K_α, θ is the diffraction angle, and β is the full width at half maximum (FWHM) (Vijayalakshmi and

Rajendran, 2012). The average crystal size was found to be 50.29 nm. Similar results were obtained for the green-synthesized Zinc Oxide nanoparticles using *Peltophorum pterocarpum* leaf extract [(Pai et al., 2019).

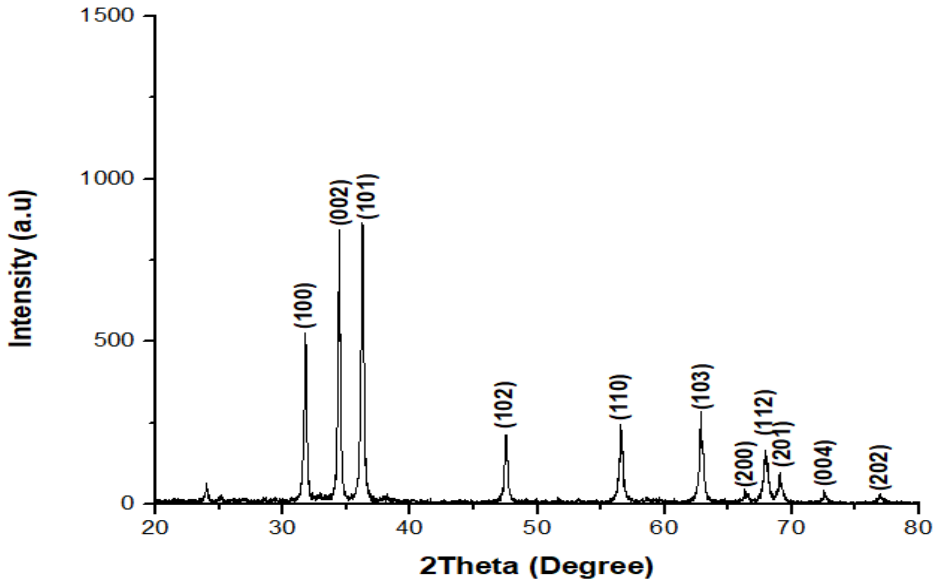

Figure 6. XRD spectra of Zinc Oxide nanoparticles.

FE-SEM analysis of ZnO NPs

FE-SEM analysis was used to evaluate the surface morphology of green-synthesized ZnO NPs, and the resulting picture is shown in Figure 7. The majority of the ZnO NPs are in nanometer size, with an average particle size of 66.93 nm and nanorod shapes. More of the particles have the same size. However, the nanoparticles are agglomerated, which is normal for the green synthesis method. Due to the large surface area of the green-synthesized nanoparticles, their strong affinities produce aggregation or agglomeration (Agarwal et al., 2017). It may be concluded that ecological considerations have a significant impact on NP stability and agglomeration. As a result, during the nanoparticle production process, NPs adhere to one another and spontaneously form asymmetrical clusters (Vidya et al., 2013a).

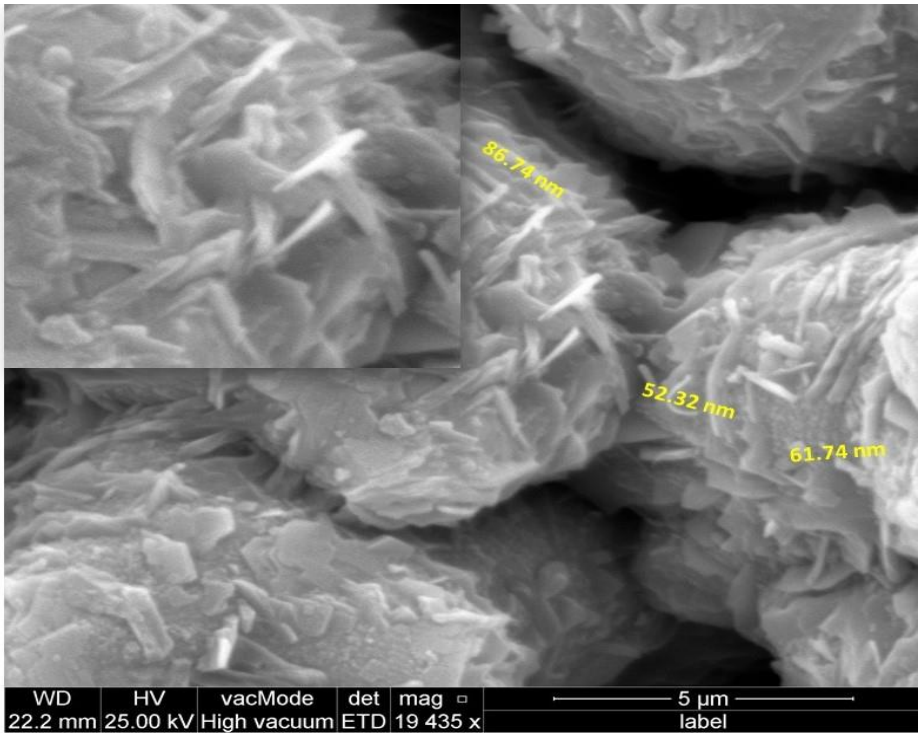

Figure 7. XRD spectra of Zinc Oxide nanoparticles.

Also, EDX analysis was used to determine the elemental analysis of the nanoparticles. The EDX spectra (Figure 8) of the ZnO NPs show that the sample contains Zinc and Oxygen elements, with weight percentages of 89.49 and 32.44, respectively. The EDX spectra exhibit two distinct zinc peaks at 1.1 keV and 8.7 keV, as well as one sharp oxygen peak at 0.5 keV, which are characteristic of ZnO NPs (Shim et al., 2019). The presence of gold is attributed to the sample being coated with a thin layer of gold during FE-SEM analysis.

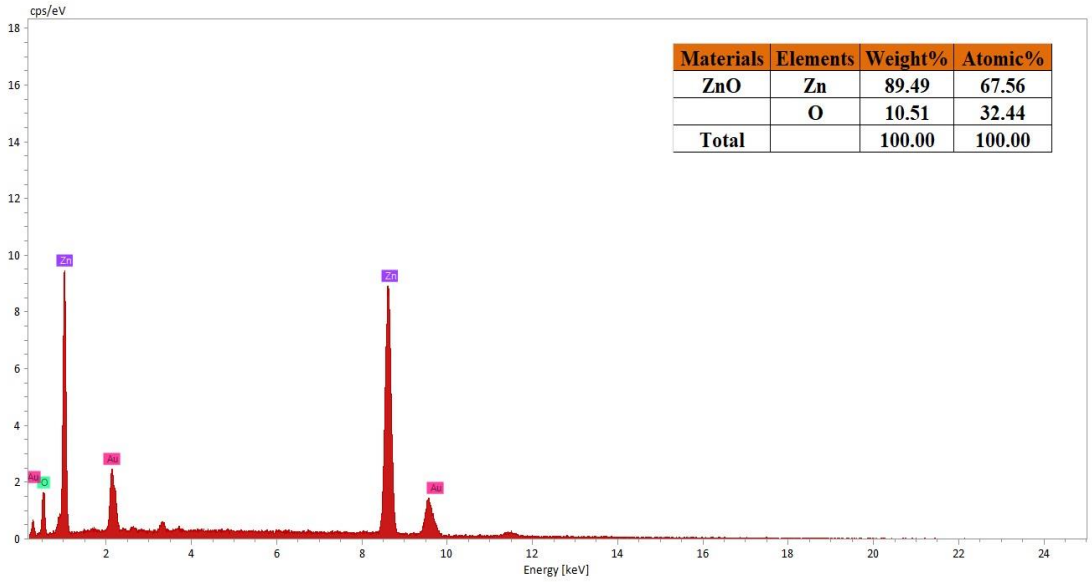

Figure 8. XRD spectra of Zinc Oxide nanoparticles.

C. Application of Synthesized Nanoparticles in Plant Growth

Morphological study:

Our results indicate significant differences in plant length between the control group and the plants treated with nanoparticle Zinc Oxide *Lepidium sativum*. The control group had a plant length of 103 mm, while the treated plants had a length of 66 mm. Furthermore, the application of Zinc Oxide NPs also affected the stem, petiole, and leaf length and width of the treated plants, as can be seen in Table 1 and Figure 9, when compared to the control group.

Table 1. Plant length, stem, and leaf dimensions of Lepidium sativum controls and those treated with ZnO NPs, in millimeters*

Plant	Plant length	Stem			Petiole			Leaf		
		length	width	A $\frac{L}{W}$	length	width	A $\frac{L}{W}$	length	width	A $\frac{L}{W}$
Control	66	(37-42) 39.5	(0.8-1.2) 1.0	39.5	(14-15) 14.5	(0.5-0.6) 0.55	26.3	(11-13) 12	(3-5) 4	3
Treated ZnO NPs	103	(56-60) 58	(1.4-1.5) 1.45	40	(20-27) 23.5	(0.8-0.9) 0.85	27.6	(13-15) 14	(6-7) 6.5	2.1

* The measurements were taken from (10-15) specimens, with the numbers inside the bracts denoting the minimum and maxi and the numbers outside the bracts denoting the average. A $\frac{L}{W}$ = Average Length/Width.

The content of vegetable dyes:

Carotenoids are a class of 750 naturally occurring dyes and non-enzyme antioxidants produced by plants in response to unfavorable environmental conditions. These compounds play a vital role in protecting cells from damage caused by free radicals. Anthocyanins, on the other hand, are water-soluble phenolic compounds that contribute to the vibrant colors seen in flowers and fruits. Chlorophyll, a natural substance found in plants, is responsible for their green color. It facilitates the absorption of solar energy and its conversion into chemical energy through the process of photosynthesis. Chlorophylls also play a role in converting magnesium ions to divalent metal ions like iron (resulting in a grey color), copper (giving a green color), or zinc (also resulting in a green shade) (MacFarlane and Burchett, 2001).

According to the results shown in Figure 10, Lepidium sativum treated with ZnO nanoparticles displayed a two-fold increase in both chlorophyll a and chlorophyll b compared to the control group. The plant cells were subjected to zinc compounds, and the levels of carotenoid and anthocyanin were measured using spectrophotometry. The studies indicated that, regardless of the form or concentration of the Zn ions, the content of carotenoids and anthocyanins increased when exposed to them, in comparison to the control sample. This finding demonstrates the activation of the plant's antioxidant system, as depicted in Figure 11.

According to tests conducted by Wang et al., a decrease in chlorophyll a, chlorophyll b, and carotenoids was observed regardless of the dose of nano-Zn used (400–32000 mg nano-Zn/kg soil). Additionally, Tiecher et al.'s research on maize showed that chlorophyll a and b levels were lower compared to control plants at all investigated dosages (30, 90, 180, or 270 mg Zn / kg soil). In contrast, Radha et al. found that sugarcane (Saccharum spp.) grown in soil with an excess amount of zinc exhibited an increase in the levels of carotenes and chlorophyll.

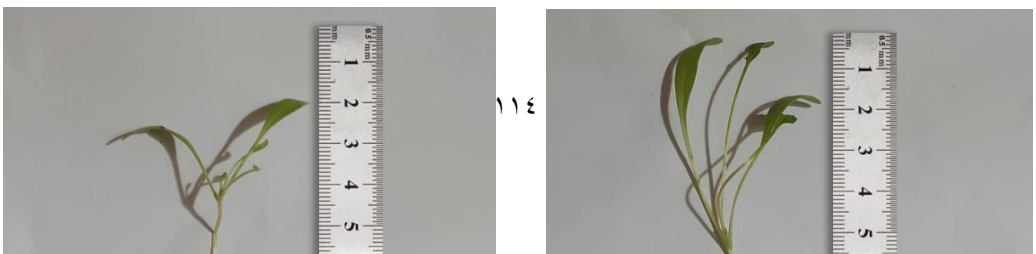

Figure 9. *Lepidium sativum* 1. Control (without ZnO NPs) and 2. Treated (with ZnO NPs).

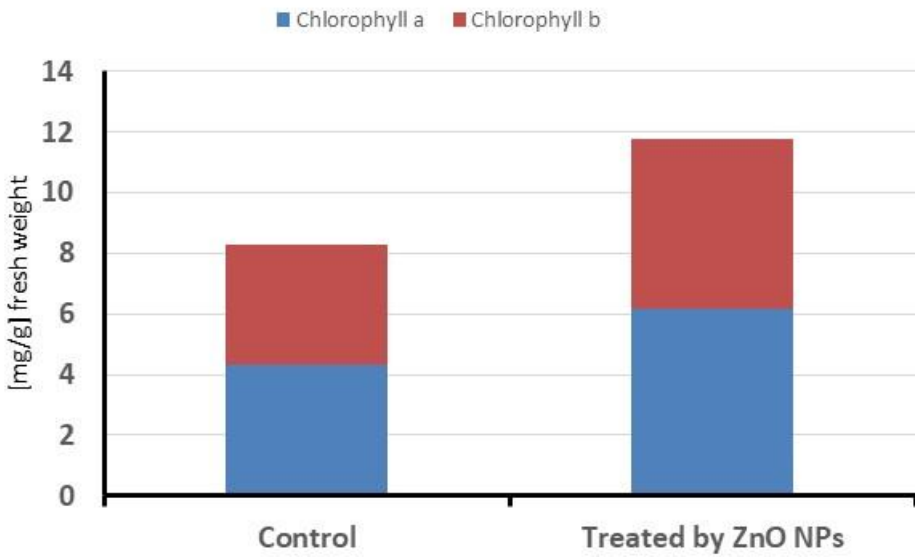

Figure 9. chlorophyll a and chlorophyll b inside plants.

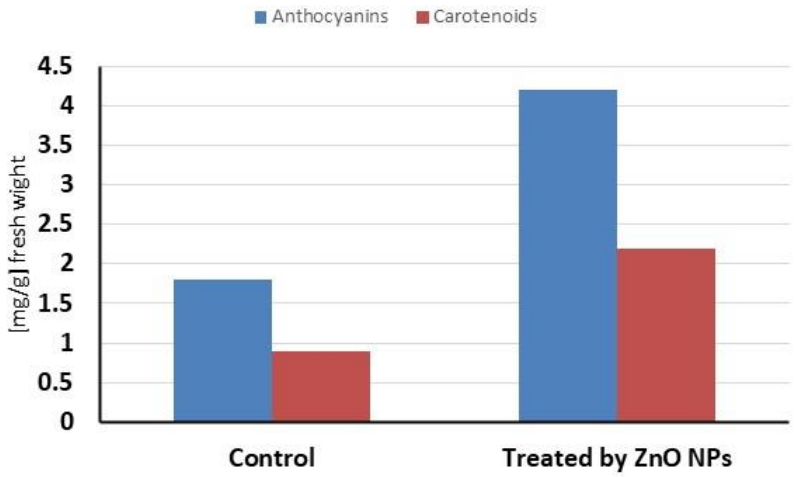

Figure 10. Concentration of carotenoids and anthocyanins for various variants of the experiment.

V. CONCLUSION

The biosynthesis of ZnO nanoparticles (NPs) using plant extract has greatly improved due to their diverse needs. This study focuses on the rapid and cost-effective production of zinc oxide (ZnO) NPs using zinc nitrate and *Artemisia abrotanum* L. aqueous leaf extract. Various techniques such as FT-IR analysis, UV-Vis spectroscopy, XRD, FE-SEM, and EDX were employed to analyze the plant components, structure, morphology, chemical composition, and optical properties of the ZnO nanoparticles. The band-gap of the ZnO NPs was calculated to be approximately 2.48 eV. However, FE-SEM revealed that the ZnO NPs have a nanorod shape with a size of 66.93 nm, and the EDX confirmed that the sample consists of pure ZnO nanoparticles. Additionally, XRD confirmed that the average crystal structure size of the ZnO NPs was 50.29 nm.

Our objective is to utilize biosynthesized ZnO NPs as an alternative to chemical fertilizers, which have adverse effects on human beings, for the growth of plants (*Lepidium sativum* L.). It has been suggested that zinc oxide nanoparticles can be used for plant cultivation instead of chemical fertilizers.

ACKNOWLEDGMENTS:

We would like to thank Salahaddin University-Erbil, as well as the Soran Research Center and Koya University, for helping us to characterize the samples during the research.

Disclosure statement:

Regarding their involvement in the research and writing of this study, the authors have not disclosed any potential conflicts of interest.

References

AGARWAL, H., KUMAR, S. V. & RAJESHKUMAR, S. 2017. A review on green synthesis of zinc oxide nanoparticles–an eco-friendly approach. Resource-Efficient Technologies, 3, 406-413.

BALA, N., SAHA, S., CHAKRABORTY, M., MAITI, M., DAS, S., BASU, R. & NANDY, P. 2015. Green synthesis of zinc oxide nanoparticles using Hibiscus subdariffa leaf extract: effect of temperature on synthesis, anti-bacterial activity and anti-diabetic activity. RSC Advances, 5, 4993-5003.

BARMAN, J. 2021. Effect of Size and pH Variation on Antibacterial Activities of ZnS-ZnO Nanocomposite Towards Application in Water Treatment. Journal of Nanostructures, 11, 654-661.

BEHZADI, M., JAROLLAHI, S., AHSANI IRVANI, M. & GHANBARI, D. 2022. Green Synthesis and Antibacterial Activity of Silver Nanoparticles Using Dracocephalum Moldavica Leaves Extract. Journal of Nanostructures, 12, 1059-1066.

BHUYAN, T., MISHRA, K., KHANUJA, M., PRASAD, R. & VARMA, A. 2015. Biosynthesis of zinc oxide nanoparticles from Azadirachta indica for antibacterial and photocatalytic applications. Materials Science in Semiconductor Processing, 32, 55-61.

DEVI, R. S. & GAYATHRI, R. 2014. Green synthesis of zinc oxide nanoparticles by using Hibiscus rosa-sinensis. International Journal of Current Engineering and Technology, 4, 2444-2446.

EVANOFF JR, D. D. & CHUMANOV, G. 2005. Synthesis and optical properties of silver nanoparticles and arrays. ChemPhysChem, 6, 1221-1231.

GANESH, M., LEE, S. G., JAYAPRAKASH, J., MOHANKUMAR, M. & JANG, H. T. 2019. Hydnocarpus alpina Wt extract mediated green synthesis of ZnO nanoparticle and screening of its anti-microbial, free radical scavenging, and photocatalytic activity. Biocatalysis and agricultural biotechnology, 19, 101129.

HEDAYATI, K. 2015. Fabrication and optical characterization of zinc oxide nanoparticles prepared via a simple sol-gel method.

HIREMATH, S., VIDYA, C., ANTONYRAJ, M. L., CHANDRAPRABHA, M., GANDHI, P., JAIN, A. & ANAND, K. 2013. Biosynthesis of ZnO nano particles assisted by Euphorbia tirucalli (Pencil Cactus). Int J Current Eng Technol (Special Issue1), 176-179.

HU, D., SI, W., QIN, W., JIAO, J., LI, X., GU, X. & HAO, Y. 2019. Cucurbita pepo leaf extract induced synthesis of zinc oxide nanoparticles, characterization for the treatment of femoral fracture. Journal of Photochemistry and Photobiology B: Biology, 195, 12-16.

ISAAC, R., SAKTHIVEL, G. & MURTHY, C. 2013. Green synthesis of gold and silver nanoparticles using Averrhoa bilimbi fruit extract. Journal of Nanotechnology, 2013.

KARIM, H. H. & OMAR, M. 2020. Temperature-dependence calculation of lattice thermal conductivity and related parameters for the zinc blende and wurtzite structures of InAs nanowires. Bulletin of Materials Science, 43, 54.

KHAN, M. M., SAADAH, N. H., KHAN, M. E., HARUNSANI, M. H., TAN, A. L. & CHO, M. H. 2019. Potentials of Costus woodsonii leaf extract in producing narrow band gap ZnO nanoparticles. Materials Science in Semiconductor Processing, 91, 194-200.

LEE, Y.-J., THIRUVENGADAM, M., CHUNG, I.-M. & NAGELLA, P. 2013. Polyphenol composition and antioxidant activity from the vegetable plant'Artemisia absinthium'L. Australian Journal of Crop Science, 7, 1921-1926.

MACFARLANE, G. & BURCHETT, M. 2001. Photosynthetic pigments and peroxidase activity as indicators of heavy metal stress in the Grey mangrove, Avicennia marina (Forsk.) Vierh. Marine pollution bulletin, 42, 233-240.

MAHDI, K. M., ALSHAMSI, H. A. & YOUSIF, Q. 2020. Graphene sheets incorporation in ZnO nanostructure thin film for enhancing the performance of DSSC. Journal of Nanostructures, 10, 793-801.

NARAYANA, A., AZMI, N., TEJASHWINI, M., SHRESTHA, U. & LOKESH, S. 2018. SYNTHESIS AND CHARACTERIZATION OF ZINC OXIDE (ZNO) NANOPARTICLES USING MANGO (MANGIFERA INDICA) LEAVES. IJRAR-International Journal of Research and Analytical Reviews (IJRAR), 5, 432-439-432-439.

OLAJIRE, A. A. & ADESINA, O. O. 2017. Green approach to synthesis of Pt and bimetallic Au@ Pt nanoparticles using Carica papaya leaf extract and their characterization. Journal of Nanostructures, 7, 338-344.

PAI, S., SRIDEVI, H., VARADAVENKATESAN, T., VINAYAGAM, R. & SELVARAJ, R. 2019. Photocatalytic zinc oxide nanoparticles synthesis using Peltophorum pterocarpum leaf extract and their characterization. Optik, 185, 248-255.

PANTIDOS, N. & HORSFALL, L. E. 2014. Biological synthesis of metallic nanoparticles by bacteria, fungi and plants. Journal of Nanomedicine & Nanotechnology, 5, 1.

REDDY, N., LI, H., HOU, T., BETHU, M., REN, Z. & ZHANG, Z. 2021. Phytosynthesis of silver nanoparticles using Perilla frutescens leaf extract: characterization and evaluation of antibacterial, antioxidant, and anticancer activities. International Journal of Nanomedicine, 16, 15.

RICHARDSON, A. D., DUIGAN, S. P. & BERLYN, G. P. 2002. An evaluation of noninvasive methods to estimate foliar chlorophyll content. New phytologist, 153, 185-194.

SADATZADEH, A., CHARATI, F. R., AKBARI, R. & MOGHADDAM, H. H. 2018. Green biosynthesis of zinc oxide nanoparticles via aqueous extract of cottonseed. J. Mater. Environ. Sci, 9, 2849-2853.

SAGAR RAUT, D. & THORAT, R. 2015. Green synthesis of zinc oxide (ZnO) nanoparticles using OcimumTenuiflorum leaves. International journal of science and research, 4, 1225-1228.

SENTHILKUMAR, N., NANDHAKUMAR, E., PRIYA, P., SONI, D., VIMALAN, M. & POTHEHER, I. V. 2017. Synthesis, anti-bacterial, antiarthritic, anti-oxidant and in-vitro cytotoxicity activities of ZnO nanoparticles using leaf extract of Tectona Grandis (L.). New J. Chem, 41, 10347-10356.

SHARMA, S., KUMAR, K., CHAUHAN, S. & CHAUHAN, M. Synthesis and Characterization of ZnO Nanoparticles using Mint Plant leaves.

SHIM, Y. J., SOSHNIKOVA, V., ANANDAPADMANABAN, G., MATHIYALAGAN, R., PEREZ, Z. E. J., MARKUS, J., KIM, Y. J., CASTRO-ACEITUNO, V. & YANG, D. C. 2019. Zinc oxide nanoparticles synthesized by Suaeda japonica Makino and their photocatalytic degradation of methylene blue. Optik, 182, 1015-1020.

VARADAVENKATESAN, T., LYUBCHIK, E., PAI, S., PUGAZHENDHI, A., VINAYAGAM, R. & SELVARAJ, R. 2019. Photocatalytic degradation of Rhodamine B by zinc oxide nanoparticles synthesized using the leaf extract of Cyanometra ramiflora. Journal of Photochemistry and Photobiology B: Biology, 199, 111621.

VIDYA, C., HIREMATH, S., CHANDRAPRABHA, M., ANTONYRAJ, M. L., GOPAL, I. V., JAIN, A. & BANSAL, K. 2013a. Green synthesis of ZnO nanoparticles by Calotropis gigantea. Int J Curr Eng Technol, 1, 118-120.

VIDYA, C., HIREMATH, S., CHANDRAPRABHA, M., ANTONYRAJ, M. L., GOPAL, I. V., JAIN, A. & BANSAL, K. 2013b. Green synthesis of ZnO nanoparticles by Calotropis gigantea. Int J Curr Eng Technol, 1, 118-120.

VIJAYALAKSHMI, R. & RAJENDRAN, V. 2012. Synthesis and characterization of nano-TiO2 via different methods. Archives of Applied Science Research, 4, 1183-1190.

YUVAKKUMAR, R., SURESH, J., SARAVANAKUMAR, B., NATHANAEL, A. J., HONG, S. I. & RAJENDRAN, V. 2015. Rambutan peels promoted biomimetic synthesis of bioinspired zinc oxide nanochains for biomedical applications. Spectrochimica Acta Part A: Molecular and Biomolecular Spectroscopy, 137, 250-258.